Energy-transfer processes in high power Yb:Tm:YLF lasers emitting at 2.3 μm

Paulo S. F.de Matos, Niklaus U. Wetter, Laércio Gomes, Márcia I. Ranieri, Sônia L. Baldocchi

Centro de Lasers e Aplicações, IPEN/SP
Av. Prof. Lineu Prestes, 2242, São Paulo 05508-000 Brazil

Abstract. Thulium has a large emission spectrum around 2.3 μm when used together with the YLF host. Since thulium concentration should be kept near 1 mol% to avoid cross-relaxation, a highly concentrated sensitizer like ytterbium is used that can be diode-pumped at 970 nm where high-power diodes are available. The population mechanism for the upper laser level includes two energy transfer up-conversion (ETU) processes from ytterbium to thulium. A third ETU process transfers population from the upper laser level. Moreover, back-transfer from thulium upper laser level to ytterbium and thulium cross-relaxation processes affect the efficiency of the 2.3 micrometer transition. Few data are available for these parameters in the literature. In this work we present experimental measurements of energy transfer parameters obtained using an OPO laser to excite selectively the energy levels. In order to establish the values and relevance of each parameter, we used a numerical, time resolved simulation which included the 5 energy levels of thulium and the 2 energy levels of ytterbium. A Yb:Tm:YLF crystal was end-pumped by a 30 W fiber coupled diode laser emitting at 973 nm. With a maximum pump power of 18 W at the crystal, 650 mW of 2.3 micrometer laser radiation were achieved in a quasi-continuous operation.

Keywords: Diode-pumped laser; rare-earth spectroscopy
PACS: 42.55.Xi

INTRODUCTION

Tunable lasers emitting around 2.3 μm are important in gas detection systems [1,2], because of the presence of strong absorption lines of atmospheric pollutants in the spectral region around 2.3 μm such as CO, CH_4 and HF. The 2.3 μm laser is used for sensing carbon monoxide and hydrocarbon gases in combustion experiments and LIDAR applications [3]. Lasers in the region of 2.0-2.5 μm are also interesting for noninvasive blood glucose measurements [4].

Thulium has large emission spectra around 2.3 μm with demonstrated tuning range of 2.2-2.45 μm using the YLF host [5]. Despite the strong absorption lines of Tm:YLF at 685 and 780 nm that are accessible with diode lasers[6], thulium is not the best choice for diode-pumping. A highly concentration dependent cross-relaxation process leads to a reduction of the 2.3 micron emission from the upper laser level and therefore, concentration should be kept below 2 mol % [5]. For efficient pump absorption, a highly concentrated sensitizer like ytterbium can be used which can be diode-pumped at 960 nm.

In the 960 nm Yb:Tm pumping scheme occur three energy transfer up-conversion (ETU) processes from ytterbium to thulium (Figure 1). After pump excitation, the ytterbium transfers its energy to the $_3H^5$ Tm level, followed by a fast multi-phonon relaxation down to the $_3F^4$ level. A second ETU process transfers energy to the $_3F^2$ energy level of thulium followed by a rapid relaxation populating the upper laser level $_3H^4$. The third ETU causes losses to the system because it transfers population from the upper laser level into the $_1G^4$ level of thulium. Back-transfer from the $_3H^4$ thulium level to $_2F^{5/2}$ ytterbium level (W5) and cross-relaxation originating from the $_3H^4$ and $_3H^6$ levels to the $_3F^4$ level (W4) deplete the upper laser level. Laser action at 2.3 micron in thulium is based on the $_3H^4$-$_3H^5$ transition.

CP992, *RIAO/OPTILAS 2007*, edited by N. U. Wetter and J. Frejlich

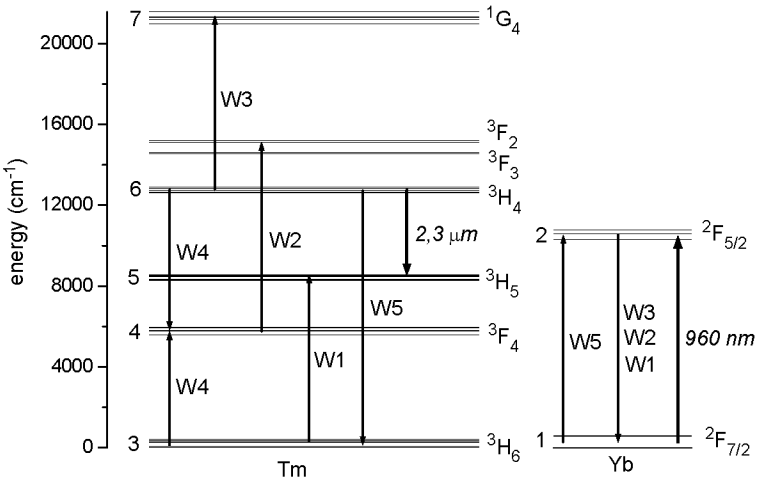

FIGURE 1. Energy-level scheme of Yb:Tm:YLF. W1, W2, W3 represent energy transfer upconversions; W4 is a cross-relaxation and W5 a back-transfer.

RATE-EQUATIONS

A numerical, time resolved simulation was used that included all energy-levels of Figure 1. The system of differential equations is solved using a fourth order Runge-Kutta algorithm. It is assumed that the crystal is longitudinally pumped. The rate equations for the population densities n_i (where the energy levels are labeled as in Figure 1) and the photon density ϕ are given by:

$$\frac{dn_1}{dt} = -R_{12} + \frac{n_2}{\tau_2} + W_1 n_2 n_3 + W_2 n_2 n_4 + W_3 n_2 n_6 - W_5 n_1 n_6 \tag{1}$$

$$\frac{dn_2}{dt} = R_{12} - \frac{n_2}{\tau_2} - W_1 n_2 n_3 - W_2 n_2 n_4 - W_3 n_2 n_6 + W_5 n_1 n_6 \tag{2}$$

$$\frac{dn_3}{dt} = \frac{n_4}{\tau_4} + \frac{\beta_{63} n_6}{\tau_6} + \frac{\beta_{73} n_7}{\tau_7} - W_1 n_2 n_3 - W_4 n_3 n_6 + W_5 n_1 n_6 \tag{3}$$

$$\frac{dn_4}{dt} = -\frac{n_4}{\tau_4} + \frac{n_5}{\tau_5} + \frac{\beta_{64} n_6}{\tau_6} + \frac{\beta_{74} n_7}{\tau_7} - W_2 n_2 n_4 + 2W_4 n_3 n_6 \tag{4}$$

$$\frac{dn_5}{dt} = R_{SE} - \frac{n_5}{\tau_5} + \frac{\beta_{65} n_6}{\tau_6} + \frac{\beta_{75} n_7}{\tau_7} + W_1 n_2 n_3 \tag{5}$$

$$\frac{dn_6}{dt} = -R_{SE} - \frac{n_6}{\tau_6} + \frac{\beta_{76} n_7}{\tau_7} + W_2 n_2 n_4 - W_3 n_2 n_6 - W_4 n_3 n_6 - W_5 n_1 n_6 \tag{6}$$

$$\frac{dn_7}{dt} = -\frac{n_7}{\tau_7} + W_3 n_2 n_6 \tag{7}$$

$$\frac{d\phi}{dt} = \frac{L_{cr}}{L_{cav}}\left(R_{SE} + f_{geo} f_{UtoL} \frac{n_6}{\tau_6} \right) + \frac{\ln(R_{out} T) c \phi}{2 L_{cav}} \tag{8}$$

where R_{SE} is the stimulated emission rate, f_{geo} is the geometrical fraction of the spontaneous emission and R_{12} is the pump rate at 975 nm given by:

$$R_{12} = \phi\left[1 - \exp\left(\sigma n_i L_{cr}\right)\right] \tag{9}$$

where σ is the effective pump absorption cross section, ϕ is the photon pump rate per volume and L_{cr} is the crystal length. The other parameters used for the numerical simulation are shown in Table 1.

The output power of the laser is calculated by:

$$P_{OUT} = \frac{(1-R_{out})c}{2}\phi\frac{hc}{\lambda_L}w_x w_y \tag{10}$$

For the numerical simulation we will use the energy-transfer parameters W_i, given in cm^6/s. W_1, W_2 and W_3 can be related to the energy-transfer probability by:

$$K_1 = n\left({}^3H_6\right)\times W_1 \tag{11}$$

$$K_2 = n\left({}^3F_4\right)\times W_2 \tag{12}$$

$$K_3 = n\left({}^3H_4\right)\times W_3 \tag{13}$$

where $n({}^3H_6)$, $n({}^3F_4)$ and $n({}^3H_4)$ are the population at these thulium levels.

TABLE 1. Parameters used for the numerical simulation.

Parameter	Symbol	Value
Laser emission cross section	σ_{em}	$1.2\text{x}10^{-20}$ cm^2
Pump absorption cross section at 975 nm [7]	σ_{ab}	$3.5\text{x}10^{-21}$ cm^2 [7]
Tm active center number density	N_{oTm}	$1.63\text{x}10^{20}$ cm^{-3}
Yb active center number density	N_{oYb}	$13.4\text{x}10^{20}$ cm^{-3}
Laser diode spot size at focus	w_x x w_y	250 x 250 μm^2
Quality beam parameter	M_x x M_y	100 x 100
975 nm pump power	P_p	20 W
Pump delivery efficiency	η_{deliv}	0.85
fluorescence lifetime $^2F_{5/2}$	τ_2	$2\text{x}10^{-3}$ s [7]
fluorescence lifetime $^3F_4$	τ_4	$15\text{x}10^{-3}$ s *
fluorescence lifetime $^3H_5$	τ_5	$1\text{x}10^{-6}$ s [7]
fluorescence lifetime $^3H_4$	τ_6	$1.2\text{x}10^{-3}$ s [8]
fluorescence lifetime $^1G_4$	τ_7	$0.74\text{x}10^{-3}$ s [7]

* measured

EXPERIMENT

We measure the energy transfer rates by pumping the crystal with an OPO. The experimental setup mainly comprises an Optical Parametric Oscillator (OPOTEK) tunable in the near infrared range from 680 to 990 nm, which delivers a typical energy of 10 mJ with a repetition rate of 10 Hz, pulse duration of 4 ns and bandwidth of 4 nm. The luminescence in the visible spectral region was collected with a refrigerated photomultiplier. For infrared measurements an InSb detector refrigerated at liquid nitrogen temperature was used. We used a 9.6 mol% Yb, 1.3 mol% Tm YLF crystal of 4.6 mm length (L_{cr}) in Brewster configuration

The same crystal used for OPO measurement was end-pumped by a 30 W fiber-coupled diode-laser emitting at 973 nm. With a maximum pump power of 18 W at the crystal, 650 mW of 2.3 micrometer laser radiation were achieved in a quasi-continuous operation. We used 8 ms pulses, 10 Hz, using a 30 cm radius-of-curvature high reflectivity input mirror and a flat output coupler with a reflectivity of 98.8%. With a maximum pump power of 18 W at the crystal, we obtained 650 mW of 2.3 micrometer laser from the 2.0 cm long cavity (L_{cav}). The temporal behavior of the output pulse was analyzed with a thermoelectrically cooled, InAs detector.

UP-CONVERSION RATES AND SIMULATION

Energy transfer probabilities and lifetimes were obtained by fitting the measured luminescence intensity curves with two exponentials:

$$I = A\left[\exp\left(\frac{-t}{t_d}\right) - \exp\left(\frac{-t}{t_s}\right)\right] \tag{14}$$

where I is the signal intensity, A its amplitude, t_s and t_d are the rise time and the decay time, respectively. Considering the intrinsic lifetime of the donor (τ_D), the rise time is calculated as:

$$\frac{1}{t_s} = K + \frac{1}{\tau_D} \tag{15}$$

where K is the energy transfer probability.

In order to calculate the first energy-transfer process K_1, the Yb:Tm:YLF crystal was excited with the OPO at 960 nm and the thulium emission was collected at 1900 nm. The thulium emissions from the $^3H_4$ energy level was obtained pumping at 975 nm and emission was collected at 800 nm. We calculated the K_1 rate as 776 s^{-1} and K_2 as 1489 s^{-1}. We can compare these transfer probabilities with data from the literature (Table 2).

TABLE 2. Transfer probabilities in s^{-1}.

Transfer probability	Measured	Reference [8]	Reference [7]
K_1	776	1255	649
K_2	1489	---	3245

Using the numerical simulation to fit the emission curves and temporal curve of the laser pulse we were able to calculate a set of transfer rates. We used the value of W5 (back-transfer) from reference [8]. Figure 2 shows the thulium emission curves measured at 1900nm and 800 nm, pumped at 975 nm and the fit for each curve calculated with the rate equation. We compare these results with reference [8] at Table 3. Figure 3 is the experimentally measured laser output and output power simulation as a function of time calculated by equation 10.

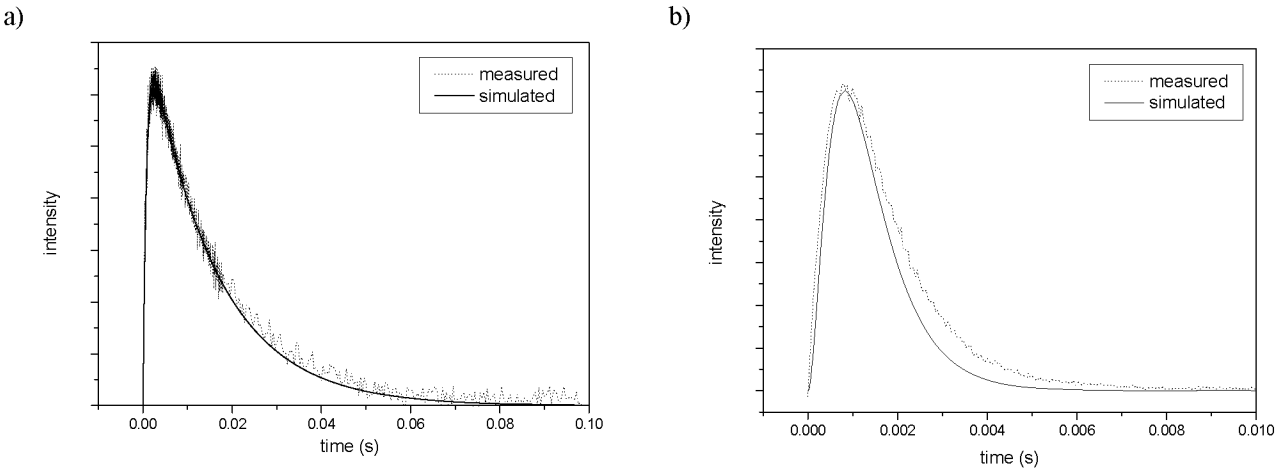

FIGURE 2. a) Thulium emission from the $^3F_4$ energy level measured at 1900 nm and the fit calculated with rate equations; b) Thulium emission from the $^3H_4$ energy level measured at 800 nm with its respective fit.

TABLE 3. Transfer rates in 10^{-18} cm^{-3} s^{-1}.

ETU	Calculated	Reference [8] *
W1 - Energy transfer upconversion 1	4.7	9.1
W2 - Energy transfer upconversion 2	30	300 or 400 **
W3 -Energy transfer upconversion 3	30	---
W4 - Cross-relaxation	16	3.2
W5 - Back-transfer	---	0.69

* 0.99 mol%Tm, 8.8 mol% Yb.
** Depends on the method.

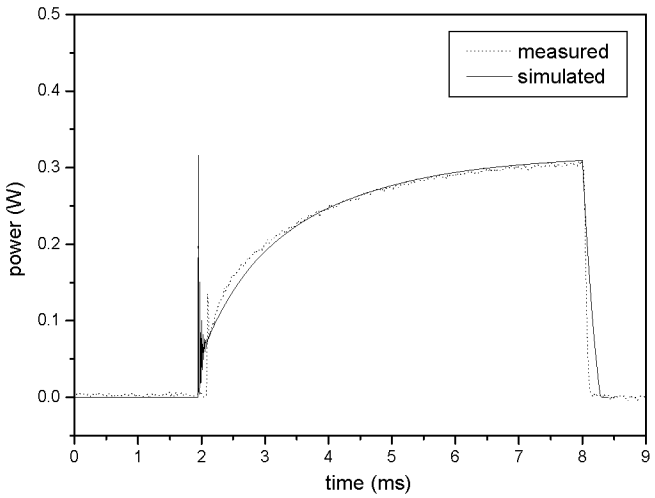

FIGURE 3. Measured and simulated output power curves.

DISCUSSION

Reference [8] considers $n(^3H_6)$ equal to the total thulium concentration and a low occupation of $^3F_4$ thulium level. As shown in Table 3, this assumption can not be justified by our calculation which is in agreement with the long life time of Tm $^3F_4$ level (15 ms). With simulation, we observed a higher population for the $^3F_4$ level than for thulium fundamental level. Comparing the transfer rates values with reference [8] (Table 3), W1 calculated by us is smaller than this reference, as K1 also is. This result is compatible with reference [7]. We calculated a W2 value 10 times smaller then that calculated by reference [8]. But this same reference present a result calculated by the Burshtein model (discarded at the article) which gives a value of 22 x 10^{-18}, much more compatible with our result.

The simulated W4 is bigger than other results from literature [7,8]. In all simulation, we noticed a necessity to use a bigger value for this cross-relaxation. This shows that for a thulium system with ytterbium, the concentration of thulium can be larger than 1 mol%, contrary to the expectation in a singly-doped, thulium system.

We also achieved a good agreement for output power curve (Figure 3) for laser in a low power regime. For high power levels, we probably need to take higher order effects into account.

CONCLUSIONS

The rate equation model shows a good agreement between numerical simulation and experimental data for a diode-pumped Yb:Tm:YLF laser emitting at 2.3 μm. We also achieved a set of energy transfer upconversion rates suitable for a numerical simulation. We demonstrate that the transfer rates W1 should be two times smaller and W2, at least 10 times smaller than previous experimental results from the literature and that our simulation results are in agreement with theoretical models from the literature. Our maximum output power of 650 mW, obtained in a qcw regime, is the highest power so far reported.

ACKNOWLEDGMENTS

We are thankful to the CNPq and FAPESP for the financial support of this work.

REFERENCES

1. F. J. McAleavey et al., *Sensors and Actuators A* **87**, 107-112 (2001).
2. L. Cerutti et al., *Phys. Stat. Sol. A* **2002** (4), 631-635 (2005).
3. M. E. Webber et al., Proceedings Of The Combustion Institute 28: 407-413 Part 1 (2000).
4. J. T. Olesberg et al., in Optical Diagnostics and Sensing V, A. V. Priezzhev and G. L. Cote, Proc. SPIE 5702, 23-29 (2005).
5. J. F. Pinto, L. Esterowitz and G. H. Rosenblatt, *Opt. Lett.* **19** (12), 683-685 (1994).
6. V. Sudesh and E. M. Goldys, JOSA B 17 (6), 1068-1076 (2000).
7. A. Diening, P. E. A. Möbert, G. Huber, *J. Appl. Phys.* **84** (11), 5900-5904 (1998)
8. A. Braud et al., *Phys. Rev. B* **61** (8), 5280-5292 (2000)